PERGAMON

Journal of Structural Geology 23 (2001) 1141–1150

JOURNAL OF STRUCTURAL GEOLOGY

www.elsevier.nl/locate/jstrugeo

Sheeting and dyking emplacement of the Gunnison annular complex, SW Colorado

B. Lafrance*, B.E. John

Department of Geology and Geophysics, University of Wyoming, PO Box 3006, Laramie, WY 82071-3006, USA

Received 12 January 1999; accepted 5 April 2000

Abstract

Emplacement of the Proterozoic Gunnison annular complex, Colorado, involved brittle failure and both subhorizontal sheeting and steeply-dipping dyking. The annular complex consists of a central diorite body (1730 Ma), surrounded by a ring of metamorphosed supracrustal rocks, in turn ringed by tonalite and granodiorite (1721 Ma). The older central diorite was emplaced as sills parallel to bedding, prior to regional deformation of the Gunnison volcanic arc, ~1730–1710 m.y. ago. This central body was deformed during regional shortening, into an upright bowl with inward-dipping walls. The surrounding country rocks were folded and locally transposed against the central body, forming an arcuate foliation, conforming roughly to the shape of the body. This foliation and bedding acted as mechanical planes of weakness, which localized the *syn*-deformational emplacement of the outer ring intrusions, as multiple magma sheets parallel to steeply dipping bedding and foliation. Portions of the outer rings were also injected along concentric, inward-dipping, shear fractures generated under high magma pressure, a process similar to cone sheet emplacement in volcanic ring-dyke complexes. Multiple mechanisms were therefore involved in the emplacement of this sheeted annular plutonic complex, which otherwise superficially resembles a subvolcanic ring-dyke complex.

1. Introduction

Sheeted plutonic complexes are igneous intrusions composed of multiple tabular igneous sheets (Hutton, 1988, 1992). During construction of these complexes, intermediate to felsic magmas, which initially rise through the crust along self-generated fractures or pre-existing faults (Clemens and Mawer, 1992; Petford et al., 1993, 1994), are emplaced as multiple sheets in dilational sites along regional faults (permissive emplacement), or are injected under high magmatic pressure along structural anisotropies under compression (forceful emplacement). The Strontian pluton in Scotland is an example of permissive emplacement of a sheeted complex in a dilational releasing bend along a strike-slip fault (Hutton, 1988), whereas forceful magmatic sheeting is exemplified by the emplacement of the sheeted Great Tonalite Sill (Alaska and British Columbia) in a contractional high-angle reverse fault zone (Hutton and Ingram, 1992). The laccolithic South Mountain batholith in Nova Scotia (Benn et al., 1997) and sheeted sills in the Chemehuevi Mountains, California (John, 1988), are other examples of sheeted plutonic complexes that formed by emplacement of granitic sheets parallel to gently-dipping structural anisotropy.

Subvolcanic ring-dyke complexes also result from the injection of magma sheets or dykes along structural discontinuities. Models for the formation of volcanic ring-dyke complexes are largely based on the pioneering work of Anderson (1936) on the island of Mull, northwest Scotland. The formation of cone sheets, ring dykes and radial dykes are functions of the stress fields in proximity to a magma chamber undergoing one or more cycles of intrusion and subsidence. During a cycle of intrusion and subsidence, pressure-buildup in the magma chamber causes shear fracturing of the country rocks (Phillips, 1974), followed by the intrusion of magma as cone sheets along the inward dipping fractures. As a consequence of the injection of magma along these fractures, pressure in the magma chamber decreases, causing subsidence of the roof rocks along outward dipping ring fractures. These fractures are subsequently infilled by magmas during subsidence of the roof, forming ring dykes. A late granite stock commonly intrudes the centre of the ring-dyke complex, ending the cycle of magmatism (Kresten, 1980; Ike, 1983).

We present the results of a detailed structural study of an

* Corresponding author. Present address: Mineral Exploration Research Centre, Department of Earth Sciences, Laurentian University, Ramsey Lake Road, Sudbury, Ontario, Canada P3E 2C6. Fax: +1-705-675-4898.

E-mail address: blafrance@nickel.laurentian.ca (B. Lafrance).

0191-8141/01/$ - see front matter
PII: S0191-8141(00)00181-4

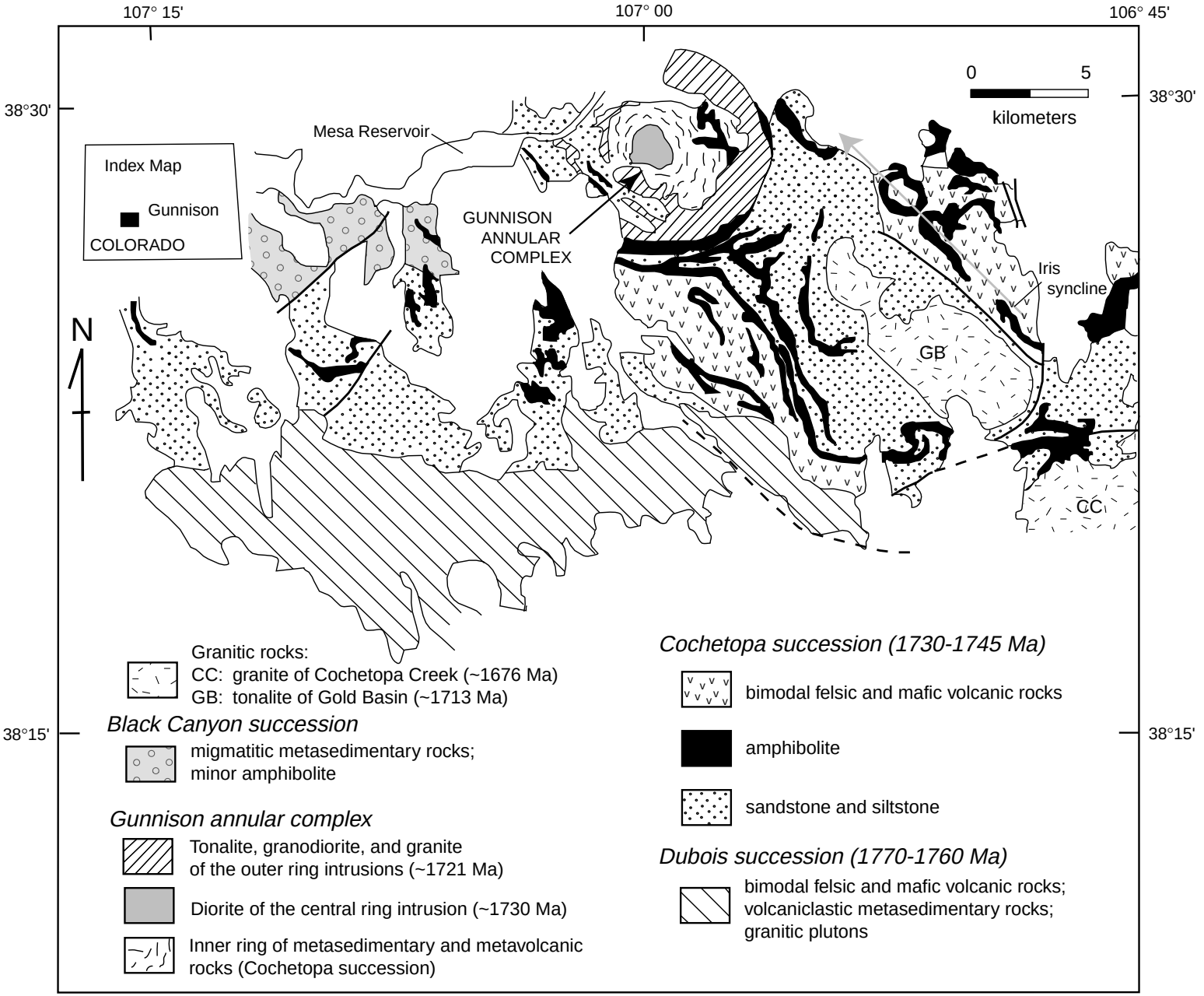
107° 15'
107° 00
106° 45'
38°30'
38°15'
0
5
kilometers
Mesa Reservoir
Index Map
Gunnison
COLORADO
GUNNISON
ANNULAR
COMPLEX
Iris
syncline
GB
CC
N
Granitic rocks:
CC: granite of Cochetopa Creek (~1676 Ma)
GB: tonalite of Gold Basin (~1713 Ma)
Black Canyon succession
migmatitic metasedimentary rocks;
minor amphibolite
Gunnison annular complex
Tonalite, granodiorite, and granite
of the outer ring intrusions (~1721 Ma)
Diorite of the central ring intrusion (~1730 Ma)
Inner ring of metasedimentary and metavolcanic
rocks (Cochetopa succession)
Cochetopa succession (1730-1745 Ma)
bimodal felsic and mafic volcanic rocks
amphibolite
sandstone and siltstone
Dubois succession (1770-1760 Ma)
bimodal felsic and mafic volcanic rocks;
volcaniclastic metasedimentary rocks;
granitic plutons

unusual plutonic complex, the Gunnison annular complex (GAC), located in the Proterozoic Yavapai Province, SW Colorado (Fig. 1). The GAC, which in map view appears as a subvolcanic ring complex, consists of an inner ring of metamorphic rocks and an outer ring of several tonalite and granodiorite intrusions, surrounding a central, sill-like, older diorite body. The emplacement history of the GAC is interesting, as it involved processes that are common to sheeted plutonic complexes (lit–par–lit magma injections parallel to pre-existing foliations), and volcanic ring-dyke complexes (magma injection along inward-dipping circular fractures). We propose an interpretation of the GAC as a sheeted plutonic complex that was emplaced during regional deformation.

2. Regional setting

Proterozoic rocks of the Yavapai Province comprise platformal cover sequences and backarc and arc terranes, which were accreted to the Archean Wyoming craton between ca. 1800–1600 Ma (Hills and Houston, 1979; Condie, 1982; Reed et al., 1987). Proterozoic rocks in the Gunnison area were deposited in oceanic and continental arc systems, south of the Wyoming craton (Bickford and Boardman, 1984; Knoper and Condie, 1988). The Gunnison rocks are divided into three sequences (Knoper and Condie, 1988; Bickford et al., 1989), namely, the Cochetopa succession (1745–1730 Ma), the Dubois succession (1770–1760 Ma), and the Black Canyon succession (Fig. 1). Both the Cochetopa and Dubois successions comprise sedimentary rocks, and bimodal volcanic and volcaniclastic deposits, metamorphosed to upper greenschist and amphibolite facies. The Black Canyon succession consists primarily of migmatitic sedimentary rocks with minor amphibolite, and is thought to be coeval with the Cochetopa succession (Knoper and Condie, 1988).

The Dubois succession was deposited in an oceanic island arc system, south of the craton (Bickford and Boardman, 1984; Knoper and Condie, 1988). It was deformed prior to the emplacement of 1751 to 1757 Ma granitic plutons (Bickford et al., 1989), presumably in response to the accretion of the arc to the growing North American continent to the north (Knoper and Condie, 1988). Renewed volcanic activity between 1745–1730 Ma led to the deposition of the Cochetopa succession on the new Gunnison continental-margin arc (Knoper and Condie, 1988).

Deformation of the Cochetopa succession occurred between 1730 Ma, the youngest depositional age of the succession, and 1713 Ma, the age of the Gold Basin tonalite (Fig. 1), a late pluton that crosscuts tectonic foliations in the Cochetopa succession (Wortman, 1991). Deformation of the continental-margin Gunnison arc between 1730 and 1713 Ma may have been caused by collision of outboard island arc terranes with the North American continent, as suggested by Ilg et al. (1996) for the Granite Gorge Metamorphic Suite in the Grand Canyon, Arizona. This suite includes 1750 to 1742 Ma, bimodal volcanic rocks, which overlap in age with the deposition of the Cochetopa succession (Ilg et al., 1996). It has a strong gneissic foliation, which developed between 1730 and 1713 Ma (Ilg et al., 1996) during the same time interval that saw the deformation of the Cochetopa succession. Alternatively, if the early Gunnison arc was separated from the North American continent by a backarc basin (Reed et al., 1987), then deformation of the older Dubois succession may have resulted from intraoceanic accretion prior to deposition of the Cochetopa succession on this intraoceanic collage. Both Dubois and Cochetopa successions were then deformed during collision of the intraoceanic collage with the craton.

The GAC was emplaced into rocks of the Cochetopa succession (Hedlund, 1974; Hedlund and Olson, 1974). Because the GAC is older than the late Gold Basin tonalite and is concordant to deformational fabrics in the Cochetopa succession, it has been interpreted as a *syn*-tectonic intrusion (Hedlund, 1974; Vance, 1984; Reed and Shropshire, 1991), possibly emplaced during arc collision, as discussed above.

3. Rock description

The 8-km-diameter GAC (Fig. 2) comprises a central diorite body dated at 1730 ± 6 Ma, an inner ring of the Cochetopa succession, and a tonalite–granodiorite outer ring dated at 1721 ± 7 Ma (U/Pb zircon, Bickford et al., 1989). Diorite xenoliths enclosed in the outer ring confirm that the central diorite body is older than the tonalite–granodiorite (Tobin, 1982). The central diorite is coarse grained with 0.5–1 cm subhedral to euhedral hornblende and plagioclase, defining a weak magmatic foliation parallel to lithological contacts. It is composed of 59.8% (±6.1%) plagioclase, 23.3% (±8.3%) hornblende, 6.7% (±5.4%) biotite, 5.8% (±1.5%) quartz, 3.6% (±2.6%) opaque minerals and 0.1% (±0.2%) K-feldspar, with minor apatite and sphene (Tobin, 1982). With decreasing hornblende and increasing quartz and biotite, the diorite grades into hornblende tonalite, which occur as multiple narrow sheets in the surrounding ring of metamorphosed country rocks. Hornblende tonalite sheets are generally less than 1 m wide, and are concordant with bedding in the metamorphic rocks. They contain abundant fine grained enclaves, rich in hornblende and biotite, and elongate parallel to the margins of the intrusions.

Fig. 1. Simplified Precambrian geologic map of the Gunnison area. Tertiary pyroclastic deposits, which locally overlie the Precambrian rocks, are not shown on the map. Mapping by Hedlund (1974), Hedlund and Olson (1974) and Vance (1984).

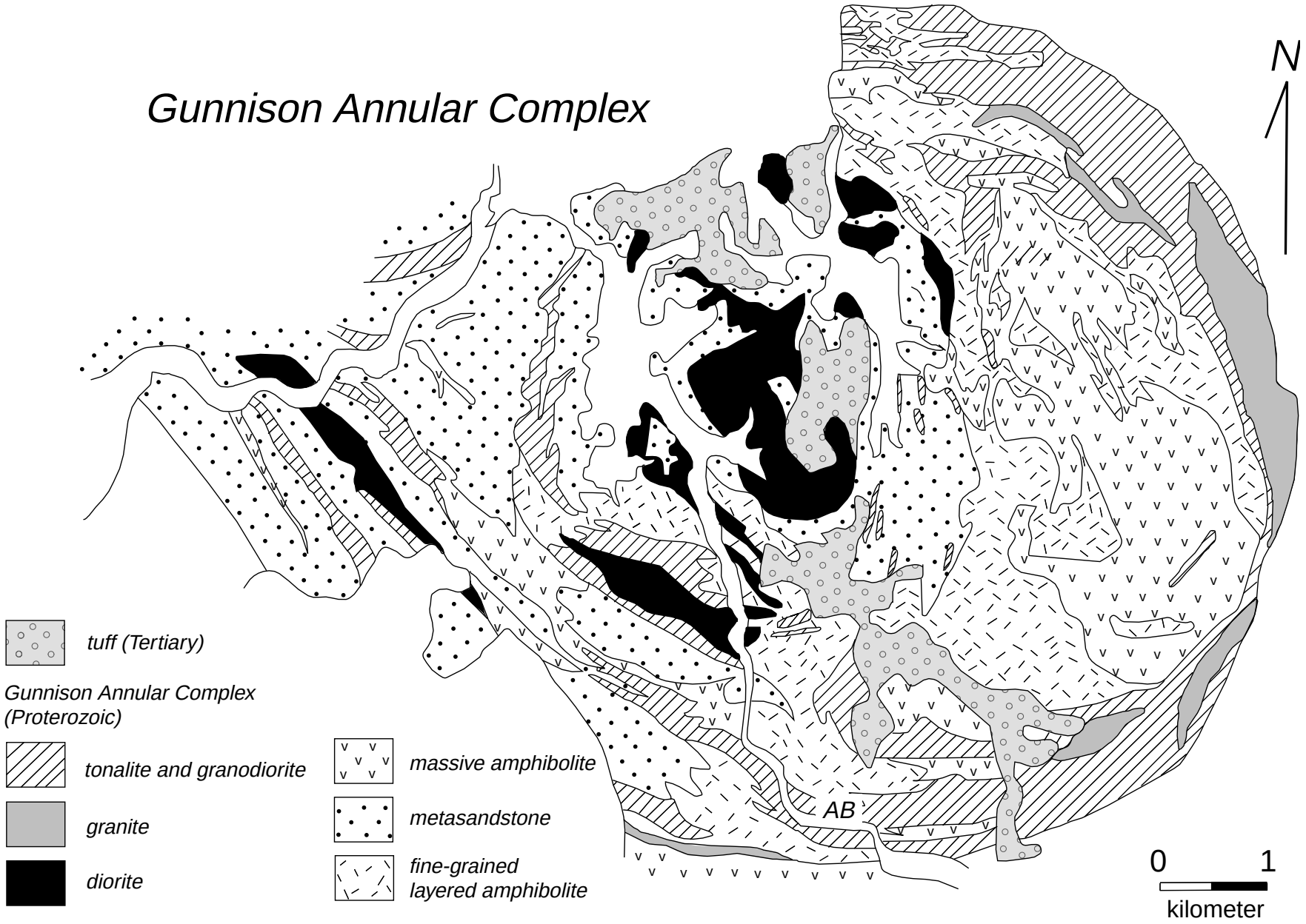

Fig. 2. Geologic map of the Gunnison annular complex. Mapping by authors.

The outer ring is made of biotite tonalite, granodiorite and granite. The biotite tonalite is fine grained, equigranular, with subhedral sodic plagioclase (Vance, 1984). It is distinguished in outcrop from the diorite to hornblende tonalite intrusions by significantly less ferromagnesian minerals, and by the pale reddish-white color. The biotite tonalite is composed of 52.9% (±7%) plagioclase, 26.8% (±7.6%) quartz, 12.4% (±4.9%) biotite, 3.3% (±6%) hornblende, 1.6% (±2.3%) microcline, opaque minerals, and minor sphene, apatite, garnet, epidote, and zircon (Tobin, 1982). With an increase in K-feldspar, the biotite tonalite grades into granodiorite, and both are in sharp contact with a pink granite that has distinctive, polycrystalline, globular quartz eyes, roughly 0.5–1 cm in diameter. Late pegmatite and aplite dykes are the youngest intrusions in the complex (Vance, 1984). The pegmatite dykes are pink-to-red on altered surfaces, and comprise large grains of quartz, microcline, plagioclase, muscovite, and biotite with minor apatite, epidote, allanite, and opaque minerals (Vance, 1984).

The inner ring of metamorphosed country rock consists of massive amphibolite, fine-grained layered amphibolite and interlayered sandstone and siltstone of the Cochetopa succession. The massive amphibolite is medium-to-coarse-grained with anhedral plagioclase and blue–green hornblende. It likely represents metamorphosed massive mafic flows or synvolcanic intrusions. The fine-grained layered amphibolite is a banded, pale green to dark green metavolcanic rock with metamorphosed clumps of feldspar, quartz, epidote, and garnet, interpreted as lapilli. The metasedimentary rocks consist of thick beds of pink sandstone (up to several meters thick) alternating with thin beds of siltstone (<1 m). Felsic metavolcanic rocks of the Cochetopa succession are chiefly ash-flow tuffs (Condie and Nuter, 1981; Knoper and Condie, 1988), but they are not exposed in the study area.

4. Structural geology

The oldest, central diorite body is a gently-dipping, sheet-like intrusion, with contacts parallel to bedding (S_0) in the host rocks both structurally above and below the intrusion. It has a magmatic foliation, defined by euhedral to subhedral plagioclase and hornblende, which are aligned parallel to the foliation. The magmatic foliation dips gently inward ($\approx$ 20–50°), parallel to the roughly circular, lower contact of the body, and is subhorizontal ($\approx$ 10–15°) in the center of the body, where it also parallels the contact with overlying metasedimentary rocks. Thus, the central diorite body has the geometry of an open, upright bowl with inward dipping walls. Other thinner diorite and hornblende tonalite sheets in the inner metamorphic ring are also concordant with S_0. They locally pinch and swell parallel to an early bedding-parallel foliation (S_1), which is defined by biotite and muscovite in sandstone and siltstone, and by hornblende and biotite in amphibolite.

Tectonic structures are best developed in the metamorphic rocks surrounding the central body. For ease of interpretation, the metamorphic ring of the GAC is divided into four structural domains (Fig. 3), based on consistent patterns of S_0/S_1 orientations (Hobbs et al., 1976). The most conspicuous structure is a macroscopic synformal F_2 fold in the SE structural domain. S_0, S_1 and thin diorite and hornblende tonalite sheets are folded by F_2. The fold has a gentle to intermediate ($\approx$ 30°) plunge near the outer margin of the ring, where it is refolded by open, S- to SW-trending F_3 folds. The F_3 folds plunge gently to the NNE and SSW, parallel to a weak axial planar S_3 foliation (Fig. 3). Closer to the central body, F_2 has a moderate-to-steep plunge ($\approx$ 60–80°); the F_3 folds become tighter, S_3 is more prominent, and the F_3 folds are locally transposed parallel to S_3. S_3 is a gneissic foliation, defined by biotite and hornblende, transposed bedding and S_1, and is accentuated by thin granodioritic to tonalitic sheets that were emplaced parallel to the foliation.

S_3 and F_3 axial planes vary systematically in orientation across the SE structural domain. S_3 and F_3 axial planes dip toward the central body, and have an arcuate N-to-NE trend, from north to south, respectively, across the domain. A down-dip stretching lineation (L_3) in S_3 plunges towards the central body. L_3 is defined by elongate biotite and hornblende grains, by stretched felsic fragments in the layered amphibolite, and by quartz-feldspar ridges alternating with biotite-rich grooves in sandstone. Adjacent to the central body, S_0 and S_1 are rotated in concordance with the margins of the central body. The foliations contain L_3, which plunges down-dip towards the body.

Similar structural relations are observed in the SW structural domain near Aberdeen Quarry ('AB' in Figs. 2 and 3), where S_0/S_1 is folded by F_3 folds, and transposed parallel to NW-trending S_3. L_3 lies in the plane of S_3 and S_0/S_1, and plunges N towards the central body. Elsewhere in the domain, L_3 plunges gently to steeply to the NW, and varies in intensity, from weak to very strong in L–S- and L-tectonites. L-tectonites that have a strong steeply-plunging lineation occur in thin metasedimentary units bounded by competent tonalitic to dioritic sheets and amphibolites. L–S-tectonites, and less commonly L-tectonites, that have an intermediate- to gently-plunging lineation, locally preserve evidence of dextral shear parallel to S_3. Shear indicators include: (1) moderately- to steeply-plunging dextral folds that deform S_3 but are themselves sheared parallel to S_3 (Fig. 4a), (2) dextral, cascade folds that are bound by S_3-parallel décollements (Fig. 4b), and that were strongly sheared to produce a geometry (Fig. 4c) similar to that of ductile dextral shear zones in rock analog experiments (Bons and Urai, 1996), and (3) sheared sigmoidal quartz lenses bounded by S_3-parallel dextral shears (Fig. 4d).

Structures in the NE structural domain have similar attitudes to those in the SW domain. S_3 trends N to NW, and S_3 and L_3 dip and plunge, respectively, to the SW

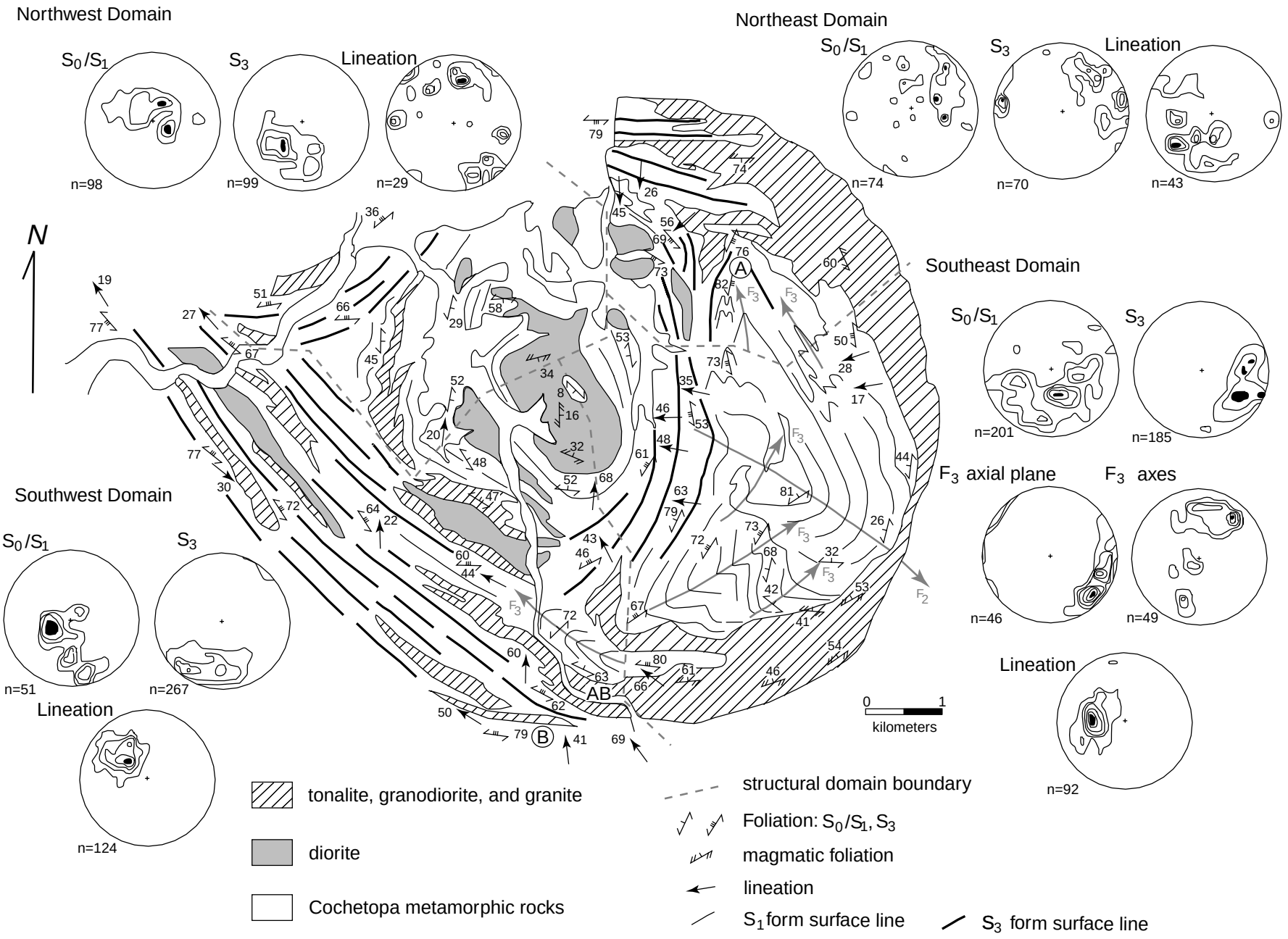
Northwest Domain
S_0/S_1
S_3
Lineation
n=98
n=99
n=29
Northeast Domain
S_0/S_1
S_3
Lineation
n=74
n=70
n=43
N
Southeast Domain
S_0/S_1
S_3
n=201
n=185
F_3 axial plane
F_3 axes
n=46
n=49
Southwest Domain
S_0/S_1
S_3
n=51
n=267
Lineation
n=124
Lineation
n=92
A
B
AB
F_2
F_3
0
1
kilometers
tonalite, granodiorite, and granite
diorite
Cochetopa metamorphic rocks
structural domain boundary
Foliation: S_0/S_1, S_3
magmatic foliation
lineation
S_1 form surface line
S_3 form surface line

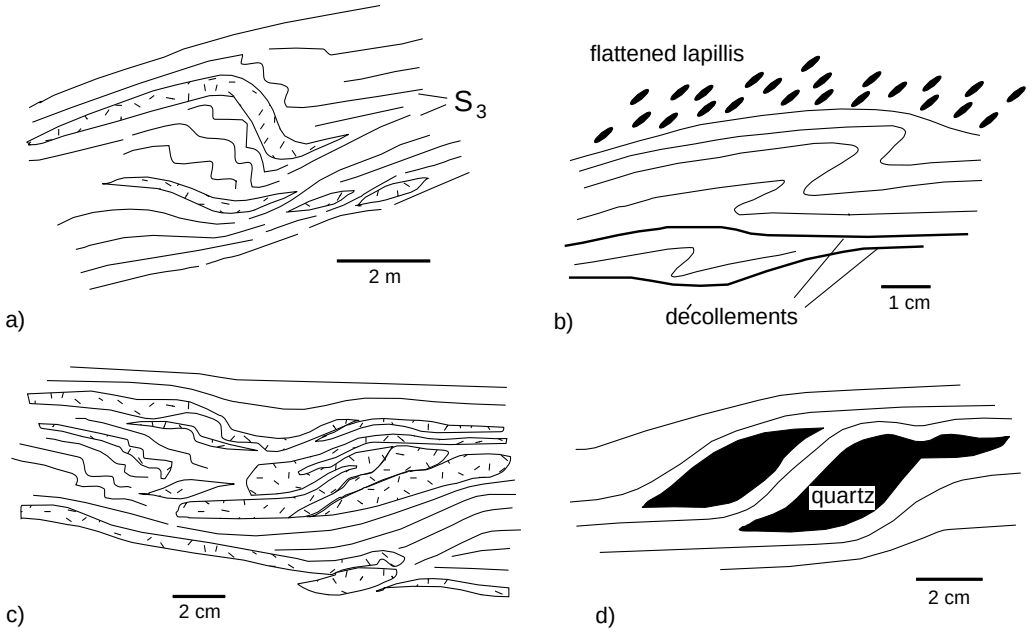

Fig. 4. Sketches of dextral shear indicators along S_3. (a) Dextral fold in psammite folding S_3, but also overprinted by S_3. (b) Cascade dextral folds bounded by S_3-parallel décollements. (c) Dextrally sheared drag folds. (d) Sigmoidal quartz lenses with dextral asymmetry. 'Stipple' pattern represents granitic dykes. Sandstone/siltstone is the main rock type in Fig. 4a–c, and layered amphibolite is the rock type in Fig. 4d.

towards the central body. In the NW structural domain, S_0 and S_1 have moderate to shallow dips toward the central body. They are folded and overprinted by E- to NE-trending S_3.

The outer ring intrusions are both concordant and discordant to S_0/S_1 and S_3. They consist of several inward-dipping intrusive sheets (40–70° dip), defining an outer circular ring cutting the metamorphic rocks. At map-scale, the circular outer ring intrusions truncate F_2 and S_0/S_1 in the SE domain, and dip more steeply than S_0/S_1. At outcrop-scale in the metamorphic ring, several thin intrusive sheets pinch and swell parallel to the arcuate, inward-dipping S_3 foliation, and inward-dipping S_0/S_1 close to the central body in the the NW and SE domains. The ring geometry partially breaks down in the SW and NE structural domains, where the intrusions are generally parallel to the NW-trending S_3 foliation, but also locally cut across the concentric S_3 foliation in the NE domain (Location 'A' in Fig. 3).

The outer ring intrusions are deformed parallel to S_3. In thin section, plagioclase commonly has patchy extinction. Plastic deformation microstructures, including deformation bands, low-angle boundaries, and undulose extinction, are observed in quartz. At map-scale in the NW domain, the outer ring intrusions are folded, and form the base of a triangular strain shadow bound on both sides by S_3 (Fig. 3). This suggests that the S_3/L_3 deformation outlasted the emplacement of the outer ring intrusions. Other tonalitic to granodioritic intrusions are Z-folded and deformed parallel to S_3 in outcrop (SW and NE domains), further suggesting that dextral shear parallel to S_3 continued after the emplacement of the outer ring intrusions. En échelon aplite and pegmatite dykes along the southern edge of the outer intrusive ring (Location 'B' in Fig. 3) cut across S_3 in a clockwise fashion, but are also Z-folded and boudinaged. The orientation of the dykes (strike 287°, dip 30° NE) with respect to S_3 (strike 270°, dip 80° N), their en échelon geometry and deformation style are consistent with the emplacement of the dykes in tension fractures in a dextral shear zone localized along the southern margin of the complex. Together, these structures suggest that the S_3/L_3 deformation ended with dextral shear parallel to S_3.

Key structural relationships are briefly summarized, as follows:

1. The central diorite body is concordant with bedding and S_1. It has the geometry of an upright bowl with inward dipping walls.
2. S_0, S_1, and diorite and hornblende tonalite sheets in the metamorphic ring are folded by a large-scale F_2 fold, which is in turn folded by F_3 folds and overprinted by S_3. F_3 folds become tighter, and S_3 is better developed, closer to the central body.

Fig. 3. Structural form surface map of the Gunnison annular complex. 'AB' refers to the location of Aberdeen Quarry; 'A' and 'B' are other locations referred to in text. The Tertiary tuff in Fig. 2 is not shown. Insets show equal-area, lower hemisphere, stereonet representations of poles to foliations (S_0/S_1, S_3) and lineations in the four structural domains of the complex. The number of measurements is on the bottom right of the stereonet diagrams. 1 and 2% area contours.

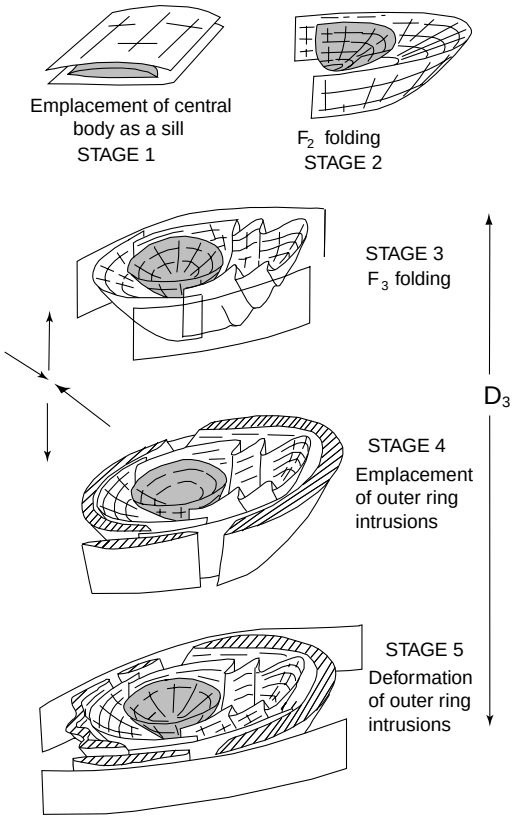

Fig. 5. Five-stage model for the development of the Gunnison annular complex. Central diorite body represented by pale gray color; outer ring intrusions by oblique-line pattern. See text for discussion.

3. A down-dip stretching lineation (L_3) plunges towards the central body around the entire GAC.
4. The outer ring intrusions are almost perfectly circular in the SW structural domain, where they truncate F_2. In the NE and SW structural domains, the intrusions are parallel and concordant to S_3.
5. In the NW structural domain, the outer ring intrusions are deformed and folded parallel to NW-trending S_3. S_3 bounds the NE and SW margins of the GAC, and has undergone dextral shear.

5. Emplacement of the Gunnison annular complex

A five-stage model is presented for emplacement of the GAC (Fig. 5). Intrusion of the GAC began at ca. 1730 Ma with the emplacement of the gently-dipping central diorite body and associated diorite and hornblende tonalite sheets as a series of concordant sills. These sheet-like bodies were intruded parallel to S_0 and S_1 (**Stage 1**) and created space for themselves by lifting the overlying beds (roof lifting).

The diorite sills, S_0 and S_1 were then folded by the NW-trending F_2 fold (**Stage 2**). This fold was first identified by Hedlund and Olson (1974), and is similar in style and orientation to the regional Iris Syncline (Afifi, 1981) to the SE (Fig. 1). Both folds have irregular profiles, presumably caused by contrasts in strength and thickness between the folded massive amphibolite and layered metasedimentary rocks. S_1 and F_2 formed during D_1 and D_2 events, respectively.

During NE-directed D_3 shortening, the central body acted as a competent body, against which the rocks of the inner metamorphic ring were folded and vertically extended. This deformation produced an arcuate S_3 foliation dipping towards the central body, and a stretching L_3 lineation plunging steeply towards the central body (**Stage 3**). This is not an uncommon occurrence in Archean and Proterozoic greenstone belts, where supracrustal rocks are tightly folded around and between more competent plutons (Windley, 1995). Continued shortening during D_3 resulted in the development of S_3 as a NW-trending foliation along both the northern and southern margins of the complex. By the end of Stage 3, the complex was surrounded by NW-trending S_3, and had the geometry of an upright cone with inward dipping foliations (S_0, S_1, S_3), surrounding a central body, itself folded as an upright bowl.

Throughout D_3, S_0, S_1, and S_3 acted as mechanical anisotropies which facilitated emplacement of the younger (1721 Ma) outer ring intrusions. The intrusions were emplaced as a series of inward-dipping magma sheets parallel to concentric S_0, S_1, S_3 around the central body, and as tabular sheets parallel to NW-trending S_3 in the SW and NE domains (**Stage 4**). Sequential compression and stress relaxation across the foliation planes (Lacroix et al., 1998) may have resulted in the permissive infilling of the foliation planes during the compressional D_3 event. Silicic magma intrusion and cooling generally occur over shorter time scales (i.e. 10,000 to 100,000 years) than regional tectonic events (i.e. several million years), so the outer ring intrusions may have been emplaced during one or more pulses of low tectonic stresses (Paterson and Tobisch, 1992). The outer ring intrusions cooled and solidified rapidly, as they are fine-grained and only weakly deformed with few plastic deformation microstructures. Pulses of low tectonic stresses may presumably result from decreases in convergence rates between colliding terranes, or from partitioning of the deformation in time and position across the terranes. Alternatively, the outer ring intrusions may have been emplaced as forceful injections if the magmatic pressure exceeded the tensile strength and tectonic stresses normal to the foliation planes. Rocks generally have low tensile strength, and rocks with structural anisotropies are even weaker (Clemens and Mawer, 1992). Even in the ductile lower crust, magma at high pressure can wedge apart foliation planes oriented normal to the maximum compressive stress (Lucas and St-Onge, 1995), thereby facilitating magmatic transport along vertical structural discontinuities. This process can also facilitate the lit–par–lit injection of magma along steep-to-horizontal structural anisotropies, producing vertically sheeted granitic

complexes (Wuluma granite, Collins et al., 1989; Lafrance et al., 1995), or horizontally sheeted laccolithic batholiths (South Mountain batholith, Benn et al., 1997). High magmatic pressure can therefore explain the emplacement of the outer ring intrusions as magma sheets parallel to pre-existing anisotropies, even if the anisotropy was oriented at high angles to compressive tectonic stresses.

Although the sheet intrusions exploited pre-existing inward-dipping foliations where possible, the almost perfectly circular shape of the eastern half of the complex can only be explained if forceful intrusions generated their own inward-dipping concentric fractures. The outer ring intrusions have a geometry similar to inward-dipping, circular cone sheets in volcanic ring dyke complexes (Anderson, 1936). However, unlike cone sheets that intrude horizontal to gently-dipping country rocks, the outer ring intrusions cut across folded and/or inclined foliations. Notwithstanding the latter observation, both outer ring intrusions in the SE structural domain and cone sheets are inward-dipping, circular, and cut across foliations, suggesting similar emplacement mechanisms. Thus, in the SE structural domain, where the outer intrusions are discordant to folded inclined foliations, the outer ring intrusions were likely emplaced as magma sheets along shear fractures (Phillips, 1974) that were generated by the upward pressure exerted by magma rising beneath the central body. The outer ring intrusions were either emplaced during a pulse of low tectonic stresses, as just discussed, or they were emplaced as several high-pressure sheet intrusions that simply overwhelmed the tectonic stresses. High-pressure magmas have been previously invoked by Parsons and Thompson (1993) as an explanation for the rotation of principal stresses during low-angle extensional normal faulting in the US Cordillera.

Later during D_3 compression, the outer ring intrusions in the NW domain and elsewhere in the complex were folded and deformed parallel to S_3, suggesting that D_3 outlasted emplacement of the GAC (**Stage 5**). The en échelon aplite–pegmatites in the dextral shear zone along the SW margin of the complex, and asymmetrical dextral shear structures along S_3, are indicative of dextral shear during D_3. D_3 is therefore a general non-coaxial deformation that comprises both S_3 perpendicular contraction and S_3 parallel dextral shear.

The five-stage model explains the geometrical and overprinting relationships between the central diorite body, the deformation structures in the metamorphic ring, and outer intrusive ring. The outer intrusive ring was emplaced during a D_3 event that began with folding and transposition of early foliations against the central diorite body, and ended with dextral shear along a strong NW-trending, S_3 foliation. Alternatively, if the concentric S_3 foliation and F_3 folds in the SE domain, and the NW-trending S_3 foliation in the NE and SW domains, formed during two different deformation events, then the outer intrusive ring could have been emplaced during a period of tectonic quiescence separating two distinct periods of deformation. This interpretation, however, is less plausible than the five-stage model presented above, as it does not explain: (1) the emplacement of outer ring intrusive sheets parallel to NW-trending S_3 in the NE and SW domains, and (2) the circular distribution of down-dip L_3 around the complex and along all foliations, including NW-trending S_3. Moreover, the five-stage model is a simpler model involving only one main deformation event (D_3), during which the outer ring intrusions were emplaced amid pulses of low tectonic stresses and/or high magmatic pressure.

Emplacement mechanisms for other annular plutonic complexes are similar to those of the GAC. The Proterozoic Ava complex in SW Finland consists of late-orogenic, inward-dipping, concentric sheet intrusions that are concordant with a gneissic ring foliation, which formed during the emplacement of an older central alkali–feldspar pluton (Branigan, 1989). In Saudia Arabia, emplacement of the Proterozoic Uyaijah ring structure was controlled by the pre-existing, funnel-shaped, magmatic foliation of the older granodiorite batholith it intruded (Dodge, 1979). The emplacement of a circular and concordant central granite, which makes up the core of the ring structure, was followed by the injection of leucogranite sheets parallel to the magmatic foliation in the older granodiorite batholith (Dodge, 1979). Thus, emplacement mechanisms of the Ava complex and Uyaijah ring structure are similar to those of the GAC, in that the outer ring intrusions exploited pre-existing foliations, within or surrounding an older pluton.

6. Conclusions

The emplacement of the GAC involves processes associated with sheeted plutonic complexes and volcanic ring-dyke complexes. As suggested by Paterson and Fowler (1993), and documented by John and Blundy (1993), several mechanisms are likely involved in the emplacement of most plutonic complexes. The lit–par–lit injection of multiple magmatic sheets, as steeply inward-dipping sheets (outer ring intrusions) and gently-dipping sills (central diorite body), parallel to pre-existing anisotropies, is remarkably similar to sheeted plutonic complexes, constructed by dyking or sheeting mechanisms. The emplacement of magma sheets along shear fractures generated by high magma pressure is a mechanism more commonly associated with volcanic ring-dyke complexes. This mechanism explains the geometry of the concentric outer ring intrusions that cut across a large-scale fold and folded foliations in the SE structural domain. However, in contrast to volcanic ring-dyke complexes, the outer ring intrusions are *syn*-tectonic, and they are concordant with pre-existing foliations elsewhere in the complex. The GAC is therefore interpreted as a sheeted annular complex that was emplaced during regional deformation.

Acknowledgements

We would like to thank A. Davidson and an anonymous reviewer for their constructive reviews, and Wouter Bleeker for his editorial comments.

References

Afifi, A.M., 1981. Precambrian geology of the Iris area, Gunnison and Saguache Counties, Colorado. M.Sc. thesis, Colorado School of Mines.

Anderson, E.M., 1936. The dynamics of the formation of cone-sheets, ring-dikes, and cauldron-subsidences. Proceedings of the Royal Society of Edinburgh 56, 128–163.

Benn, K., Horne, R.J., Kontak, D.J., Pignotta, G.S., Evans, N.G., 1997. Syn-Acadian emplacement model for the South Mountain batholith, Meguma Terrane, Nova Scotia: magnetic fabric and structural analyses. Geological Society of America Bulletin 109, 1279–1293.

Bickford, M.E., Boardman, S.J., 1984. A Proterozoic volcano-plutonic terrane, Gunnison and Salida areas, Colorado. Journal of Geology 92, 657–666.

Bickford, M.E., Shuster, R.D., Boardman, S.J., 1989. U-Pb geochronology of the Proterozoic volcano-plutonic terrane in the Gunnison and Salida areas, Colorado. Geological Society of America Special Paper 235, 33–48.

Bons, P.D., Urai, J.L., 1996. An apparatus to experimentally model the dynamics of ductile shear zones. Tectonophysics 256, 145–164.

Branigan, N.P., 1989. Hybridization in Middle Proterozoic high-level ring complexes, Aland, SW Finland. Precambrian Research 45, 83–95.

Clemens, J.D., Mawer, C.K., 1992. Granitic magma transport by fracture propagation. Tectonophysics 204, 339–360.

Collins, W.J., Flood, R.H., Vernon, R.H., Shaw, S.E., 1989. The Wuluma granite, Arunta Block, central Australia: an example of in situ, near-isochemical granite formation in a granulite-facies terrane. Lithos 23, 63–83.

Condie, K.C., 1982. Plate-tectonics model for Proterozoic continental accretion in the southwestern United States. Geology 10, 37–42.

Condie, K.C., Knoper, J.A., 1981. Geochemistry of the Dubois greenstone succession: an early Proterozoic bimodal volcanic association in west-central Colorado. Precambrian Research 15, 131–155.

Dodge, F.C.W., 1979. The Uyaijah ring structure, Kingdom of Saudia Arabia. US Geological Survey Professional Paper 774-E, 17p.

Hedlund, D.C., 1974. Geologic map of the Big Mesa quadrangle, Gunnison County, Colorado. US Geological Survey Geologic Quadrangle Map GQ-1153, scale 1:24,000.

Hedlund, D.C., Olson, J.C., 1974. Geologic map of the Iris NW quadrangle, Gunnison and Saguache Counties, Colorado. US Geological Survey Geologic Quadrangle Map GQ-1178, scale 1:24,000.

Hills, F.A., Houston, R.S., 1979. Early Proterozoic tectonics of the central Rocky Mountains, North America. University of Wyoming Contributions to Geology 17, 89–109.

Hobbs, B.E., Means, W.D., Williams, P.F., 1976. An Outline of Structural Geology. John Wiley & Sons, New York.

Hutton, D.H.W., 1988. Granite emplacement mechanisms and tectonic controls: inferences from deformation studies. Transactions of the Royal Society of Edinburgh: Earth Sciences 79, 179–190.

Hutton, D.H.W., 1992. Granite sheeted complexes: evidence for the dyking ascent mechanism. Transactions of the Royal Society of Edinburgh: Earth Sciences 83, 377–382.

Hutton, D.H.W., Ingram, G.M., 1992. The Great Tonalite Sill of southeastern Alaska and British Columbia: emplacement into an active high angle reverse shear zone (extended abstract). Transactions of the Royal Society of Edinburgh: Earth Sciences 83, 383–386.

Ike, E.C., 1983. The structural evolution of the Tibchi ring-complex: a case study for the Nigerian Younger Granite Province. Journal of the Geological Society of London 140, 781–788.

Ilg, B.R., Karlstrom, K.E., Hawkins, D.P., Williams, M.L., 1996. Tectonic evolution of Paleoproterozoic rocks in the Grand Canyon: Insights into middle-crustal processes. Geological Society of America Bulletin 108, 1149–1166.

John, B.E., 1988. Structural reconstruction and zonation of a tilted mid-crustal magma chamber: the felsic Chemehuevi Mountains plutonic suite. Geology 16, 613–617.

John, B.E., Blundy, J.D., 1993. Emplacement-related deformation of granitoid magmas, southern Adamello Massif, Italy. Geological Society of America Bulletin 105, 1517–1541.

Knoper, M.W., Condie, K.C., 1988. Geochemistry and petrogenesis of early Proterozoic amphibolites, west-central Colorado, USA. Chemical Geology 67, 209–225.

Kresten, P., 1980. The Alnoi complex; tectonics of dike emplacement. Lithos 13, 153–158.

Lacroix, S., Sawyer, E.W., Chown, E.H., 1998. Pluton emplacement within an extensional transfer zone during dextral strike-slip faulting: an example from the late Archean Abitibi Greenstone Belt. Journal of Structural Geology 20, 43–59.

Lafrance, B., Clarke, G.L., Collins, W.J., Williams, I.S., 1995. The emplacement of the Wuluma granite: melt generation and migration along extensional fractures at the close of the Late Strangways orogenic event, Arunta Block, central Australia. Precambrian Research 72, 43–67.

Lucas, S.B., St-Onge, M.R., 1995. Syn-tectonic magmatism and the development of compositional layering, Ungava Orogen (northern Québec, Canada). Journal of Structural Geology 17, 475–491.

Parsons, T., Thompson, G.A., 1993. Does magmatism influence low-angle normal faulting? Geology 21, 247–250.

Paterson, S.R., Fowler, K.T., 1993. Re-examining pluton emplacement processes. Journal of Structural Geology 15, 191–206.

Paterson, S.R., Tobisch, O.T., 1992. Rates of processes in magmatic arcs: implications for the timing and nature of pluton emplacement and wall rock deformation. Journal of Structural Geology 14, 291–300.

Petford, N., Kerr, R.G., Lister, J.R., 1993. Dike transport of granitoid magmas. Geology 21, 845–848.

Petford, N., Lister, J.R., Kerr, R.C., 1994. The ascent of felsic magmas in dykes. Lithos 32, 161–168.

Phillips, W.J., 1974. The dynamic emplacement of cone sheets. Tectonophysics 24, 69–84.

Reed, J.C., Shropshire, K.L., 1991. Early Proterozoic volcanogenic sequences in central Colorado. Colorado Scientific Society, Fall field trip.

Reed, J.C., Bickford, M.E., Premo, W.R., Aleinikoff, J.N., Pallister, J.S., 1987. Evolution of the Early Proterozoic Colorado province: Constraints from U-Pb geochronology. Geology 15, 861–865.

Tobin, R.J., 1982. Petrology and geochronology of a Proterozoic annular plutonic complex near Gunnison, Colorado. M.Sc. thesis, University of Kansas.

Vance, R.K., 1984. Geology and geochemistry of the Gunnison intrusive complex, Gunnison county, Colorado. M.Sc. thesis, University of Kentucky.

Windley, B.F., 1995. The Evolving Continents. John Wiley & Sons, Chichester.

Wortman, G.L., 1991. Time relationships among deformation, metamorphism, and plutonism in the early Proterozoic of Colorado. M.Sc. thesis, University of Kansas.